Speed of Response, Pile-up and Signal to Noise Ratio

in Liquid Ionization Calorimeters

WALIC collaboration

presented by

J. Colas

L.A.P.P., Annecy-le-Vieux, 74019 France

Summary: Although liquid ionization calorimeters have been mostly used up to now with slow readout, their signals have a fast rise time. However, it is not easy to get this fast component of the pulse out of the calorimeter. For this purpose a new connection scheme of the electrodes, the "electrostatic transformer", is presented and discussed. This technique reduces the detector capacitance while keeping the number of channels at an acceptable level. Also it allows the use of transmission lines to bring signals from the electrodes to the preamplifiers which could be located in an accessible area. With room temperature liquids the length of these cables can be short, keeping the added noise at a reasonable level. Contributions to the error on the energy measurement from pile up and electronics noise are studied in detail. Even on this issue, room temperature liquids (TMP/TMS) are found to be competitive with cold liquid argon at the expense of a moderately higher gap voltage.

1. Introduction

The new generation of high energy hadron colliders (LHC/SSC) presents an experimental challenge for detectors. The short time interval between bunch crossings (≈ 15 ns) stresses the need for fast devices. Calorimeters will play an important role in these detectors as their resolution improves with increasing energy.

Among the various calorimetry techniques, liquid ionization detectors are strong candidates for their known stability in time and their ease of segmentation. However questions arise : are they fast enough to keep pile up under control ? How large is the electronics noise at the very short shaping times which are required at LHC/SSC ? In a previous paper [1] Radeka and Rescia studied these problems and, based on their experience with the fast liquid argon calorimeter built by the Helios collaboration [2], showed that although non trivial, the use of liquid argon calorimeters at LHC/SSC is feasible if certain constraints are obeyed. A slightly different analysis has also been made by Franzini[3].

This paper revisits these questions with emphasis on the use of room temperature liquids (TMP/TMS). It presents a new technical solution to speed up calorimeter readout and through explicit computation compares performances expected for TMP/TMS and liquid argon.

This work is part of a more general effort by the WALIC collaboration [4] to study room temperature liquids (TMP/TMS) as possible alternative to cold liquid argon as sensitive medium in sampling calorimeters. Room temperature liquids require neither cryogenic equipment nor thermal insulation, resulting in a simpler and more hermetic detector. A detailed study is presently being made to quantify this point. Furthermore, since room temperature liquids are hydrogenuous materials, they may provide a compensated output, that is, a nearly equal response to electromagnetic and hadronic showers, leading to better resolution and linearity over a large energy range, without having to resort to expensive and exotic materials. Measurements on the saturation properties of TMP/TMS which are important for this compensation mechanism to occur have been done by the WALIC collaboration and reported at this conference [5]. A modular hadronic calorimeter, specially designed to study compensation is presently being built and direct measurements will be made in a test beam at Fermi Lab in 1990. These attractive features have to be balanced by the purity requirement of the liquids. If the UA1 collaboration has solved the problem of producing large quantity of very clean liquid where electrons can drift for more than 100 μs [6], too little is known up to now about materials which can be used in direct contact with the liquid. R&D is also going on in that direction.

2. Basic features of the signal formation in ionization chambers

The drift of the ionization electrons in the inter electrode gap of a sampling calorimeter under the influence of an external electric field induces a current signal. Usually, the drift velocity of the ions is so small that as, we will see below, their current pulse can be ignored. Assuming a uniform ionization through the gap, the moving electron charges produce the triangular shaped current pulse shown in figure 1. Its main characteristics are:

i)   A fast rise time. Usually the gap size is small and propagation effects can be ignored.

ii) The peak current I_{max} is a function of the density of ionization and of the drift velocity v_d only :

$$I_{max} = G_{fi} \times \frac{dE}{dx} \times v_d$$

where G_{fi} the free ion yield measures the number of electron ion pairs produced per unit of energy loss and dE/dx is the energy loss per unit length in the liquid. Typical values of G_{fi}, dE/dx, v_d and I_{max} are [1,7,8]:

Liquid	dE/dx MeV/cm	G_{fi} 1/100 eV	v_d mm/μs	I_{max} ke/μs
liquid argon@10kV/cm	2.11	3.8	5.0	40.5
TMP@40kV/cm	1.58	2.0	11.6	36.9
TMS@20kV/cm	1.36	1.6	19.6	46.3

iii) The drift-time t_d which is the time an electron takes to cross the whole gap (g). At this point in time the current returns to 0.
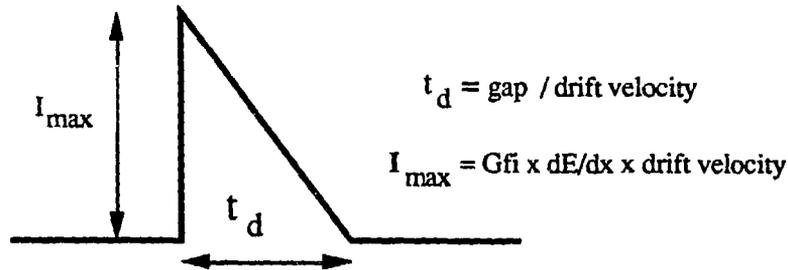
$$t_d = \frac{g}{v_d}$$

2

Figure 1 . Induced current waveform in ionization chambers for a uniform energy deposition in the interelectrode gap. t_d is the electron drift time across the gap. G_{fi} is the free electron yield per unit of energy lost in liquid and dE/dx is the energy loss by ionization per unit length.

In most of the existing liquid ionization calorimeter, the drift time is much smaller than the measurement time and the quantity of interest is the total charge collected onto the electrodes :

$$Q = \frac{1}{2} \times I_{max} \times t_d = \frac{1}{2} \times G_{fi} \times \frac{dE}{dx} \times g$$

This will not be the case in an LHC/SSC calorimeter, and the two quantities I_{max} and t_d have to be considered separately. They both depend on the drift velocity. The larger the drift velocity, the larger the peak current and the smaller the drift time. This is why ions with their very low velocities are not detected. Figure 2 shows drift velocities for several liquids as a function of the electric field [1,7]. In liquid argon the drift velocity saturates above ≈ 5 KV/cm. Saturation is less when it is doped with CH4, and even less for room temperature liquids where the drift velocity compares favorably with that of liquid argon at high electric field. For TMP these data are consistent with what has been measured by UA1 [8] and by WALIC up to 25 kV/cm . For TMS, a new measurement [9] indicates an even higher drift velocity above 20 kV/cm.

Three questions then come to mind if we want to build a fast liquid ionization calorimeter :

i)   Can we take advantage of the fast rise time of the current waveform to get a fast pulse out of the calorimeter?
ii) Drift time will probably be longer than the 15 ns between bunch crossings. How does that affect the pile-up from one collision to the next one?
iii) What kind of signal to noise ratio can we expect at the small shaping time we want to use at LHC/SSC?

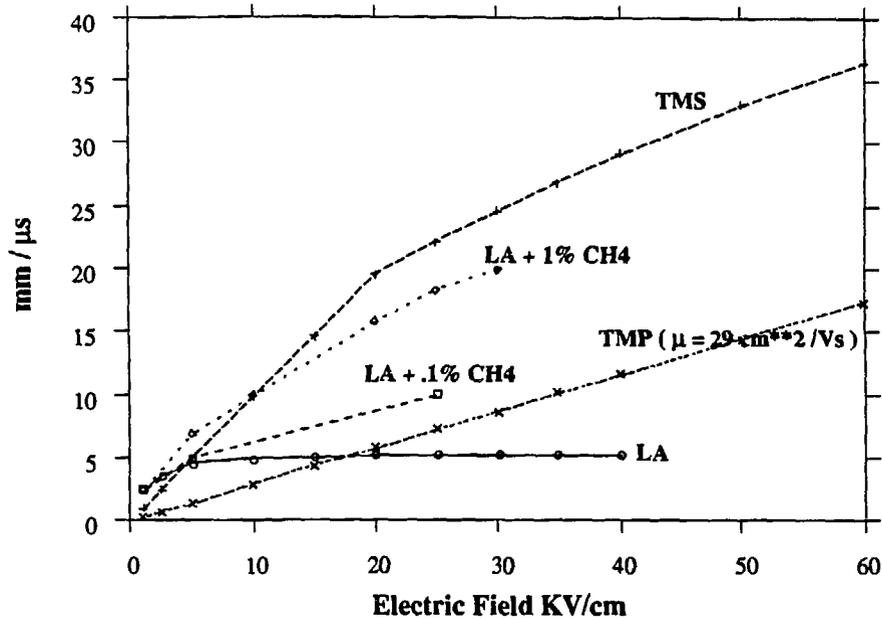Each of these points will be developed in the following sections.

Figure 2. Drift velocities for various liquids as function of the drifting electric field. In room temperature liquids drift velocities saturate at much higher electric field than in liquid argon.

3. Fast Calorimeter Read-out

As discussed in reference 1, the electric characteristics of the circuit formed by the ionization chamber and its preamplifier can be summarized in the schematic of figure 3. The ionization current is forced by the driving electric field to charge the capacitance made up of the detector plates and the electrical connections. This capacitance discharges itself through the self inductance of the connections to the input resistance of the preamplifier which provides the necessary damping.

$$\tau_1 = R * C$$
$$\tau_2 = \sqrt{L * C}$$
$$\tau_3 = L / R$$

Include detector
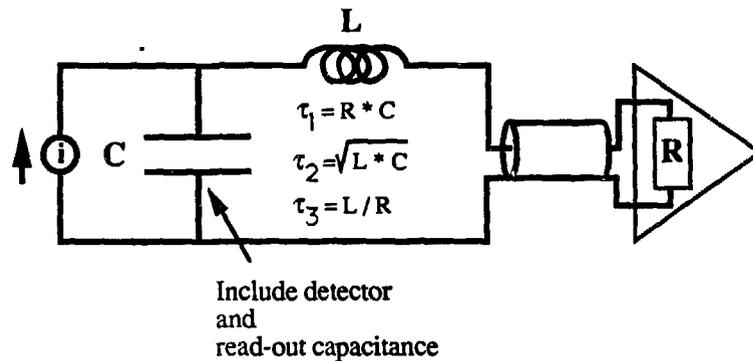and
read-out capacitance

Figure 3. Equivalent circuit of a liquid ionization cell connected to its preamplifier. To damp oscillations, the input impedance of the preamplifier is made resistive and the time constant τ_1 has to dominate over the others. A transmission line connecting the detector cell to the preamplifier does not change the picture if its impedance is matched to the preamplifier input resistance.

Of the three time constants of the circuit :

$$\tau_1 = RC, \quad \tau_2 = \sqrt{LC}, \quad \tau_3 = L/R$$

the first one has to be dominant if one wants to minimize ringing. The critical damping condition is met for $\tau_1 = 2\tau_2 = 4\tau_3$. The rise time of the pulse [10% - 90%] at the preamplifier level, which can be looked at as the charge transfer time, is then $\approx 2\,RC$. A transmission line between the detector and the preamplifier if properly terminated by its characteristic impedance, does not change the picture and just acts as delay line. In most of the present liquid ionization calorimeters C is of order 5 nF and R of order 50 Ω which implies a $\approx$ 500 ns charge transfer time. This has to be contrasted with the 15 ns spacing between bunch crossings expected at LHC/SSC.

There are two known ways out to improve the charge transfer time :

i- Reduce the damping resistor. This is for instance the case in the Helios calorimeter at CERN [2], where a ferrite transformer is used to lower the input resistance of the preamplifier to $\approx$ 3 Ω, leading to a rise time of less than 50 ns [1]. In this case the use of low impedance transmission lines is not practical; they become too bulky and in addition they add too much noise due to their large capacitance. The preamplifiers have to be on the electrodes, as in Helios. The next limitation comes from the self-inductance of the connections. The damping resistor is so small that the time constant L/R is not negligible and oscillations may occur.

ii- Reduce the tower capacitance. If we can keep the tower capacitance below say 300 pF, then a damping resistor of $\approx$75 Ω which gives a charge transfer time of $\approx$ 45 ns is perfectly acceptable from the point of view of speed but also leads to a reasonable impedance for a transmission line. In addition, with a lower tower capacitance, the self inductance of all the connections are less critical than in the previous solution. The standard way to achieve such a reduction in capacitance is by decreasing the pad surface or the number of gaps connected in parallel. This is what will occur in the electromagnetic section of a highly segmented calorimeter. If we consider a segmentation $\Delta\eta \times \Delta\phi = .03 \times .03$ [10], a typical electromagnetic sampling with all gaps connected in parallel will have a capacitance of order 330 pF. There is a large number of towers $\approx$ 40,000 over the interval of rapidity $|\eta|<3$ and an even greater number of preamplifiers $\approx$ 120,000, one per sampling in depth. However such a method applied to the hadronic part of the calorimeter leads to an unreasonable number of channels. Assuming a spatial resolution $\Delta\eta \times \Delta\phi = .05 \times .05$ i.e. 15,000 towers over the whole rapidity region $|\eta|<3$, we would need $\approx$ 75 samplings in depth, i.e. $\approx$ 1,100,000 preamplifiers, to keep the sampling capacitance within the 300 pF limit !

A possible alternative to reduce the capacitance of large hadronic towers is to gang the drifting gaps in series rather than in parallel. This is what we call the electrostatic transformer approach (EST) as it behaves from the preamplifier point of view very much the same as a ferrite-core transformer. The idea is sketched in figure 4, where series connection is compared to parallel ganging, and more fully developed in reference 11. The drawbacks of this solution -- possibly higher high voltage, non uniformity in the gap collection efficiency and increased cross-talk from adjacent calorimeter towers -- are discussed in the next section. In the previous example, using a transformer ratio of 3 would reduce the number of necessary preamplifiers by nearly an order of magnitude.

In conclusion, even if the current coming out of the drifting gaps has a fast rise time, it is non trivial to extract this fast component from the calorimeter due to the capacitive nature of ionization detectors. There is one known way, which has been demonstrated successfully by the Helios collaboration, using ferrite-core transformers
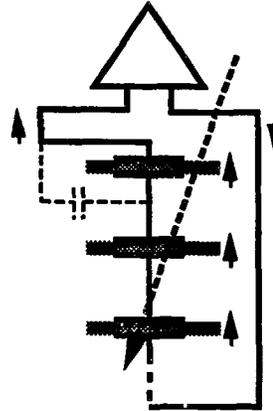
a) Parallel connection

b) Series connection
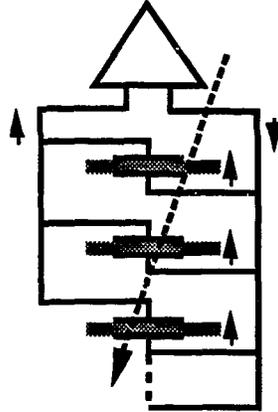
$$C_{tot} = p \times C_{gap}$$
$$I_{tot} = p \times I_{gap}$$
$$Signal / Noise \approx \sqrt{p}$$

$$C_{tot} = C_{gap} / s$$
$$I_{tot} = <I_{gap}>$$
$$Signal / Noise \approx \sqrt{s}$$

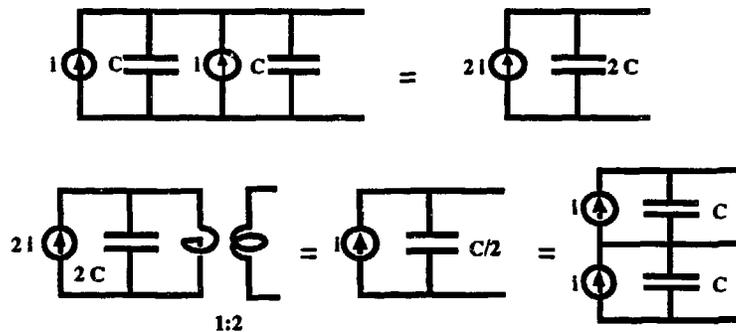## c) Equivalence between a ferrite transformer and an EST

Figure 4. Comparison of the parallel and series connection (EST) of several gaps. In the parallel case, the equivalent current source is the sum of the current in each gap (p in total). The total capacitance seen by the preamplifier is the sum of the capacitance of each gap. A ferrite transformer of turn ratio p transforms this into a current <I> and a capacitance C/p. In the series connection, the equivalent current source is the average current of the gap currents <I>. The capacitance seen by the preamplifier is the gap capacitance divided by the number of gaps in series (s in total) C/s. This much smaller capacitance allows a faster readout. In a mixed scheme, some of the gaps would be connected in parallel and some in series. Note, that in both cases, energy conservation implies that the same signal to noise ratio is achievable.

6

and preamplifiers close to the electrodes. Another alternative using the EST approach of connecting several gaps in series allows the use of transmissions lines to transport signals from the electrodes to preamplifiers located outside of the calorimeter in an accessible area. To keep the added noise to a reasonable level, these cables should be short (≤ 5 m) which seems feasible in a room temperature liquid calorimeter.

4. The ElectroStatic Transformer.

Two designs of a calorimeter tower are shown schematically in figure 4. In both, absorbing electrodes are separated by liquid sensitive gaps. Ionization electrons produced by shower particules are collected with the help of a large voltage gradient. In other respects the designs are very different. Figure 4a shows the traditional ganging; all the signal gaps are connected in parallel and the individual gap currents are summed. Figure 4b shows an alternative in which the gaps are connected in series. The gap currents are not directly summed but the average signal is delivered on a much higher impedance. And because as seen from the preamplifier this performs the same signal and impedance transformation as the ferrite-core transformer (figure 4c), we have called it the ElectroStatic Transformer (EST). A mixed scheme in which subsets of gaps within a tower are connected in series will probably turn out to be more practical; in all cases, a large reduction in the tower capacitance is obtained. As an example, a typical hadronic tower with 40 gaps of 250 pF each has a total capacitance of 10 nF if all gaps are connected in parallel, but only 0.4 nF if the stack is structured in 8 parallel sets of 5 gaps in series each. In such a scheme, the number of gaps in series plays the same role as the turn ratio in a ferrite-core transformer and has been given the same name: transformer ratio.

4.1 High voltage connection

Figure 4 implies that the d.c. voltages in adjacent gaps of the EST are connected in series. This is conceptually straightforward, but would require an uncomfortably high voltage. In alternative designs, the gaps are decoupled individually so that the maximum voltage is no greater than that across each gap. The example shown conceptually in figure 5 uses metallic tile absorbers imbedded in thin insulating layers. Facing the absorber tiles are metallized pads on the surface of the insulator, resistively connected horizontally to neighbors and eventually to the high voltage source. High voltage decoupling occurs via the capacitances between pads on opposite sides and absorber. Such a structure has the nice features that high voltage is fed in parallel, signal is readout in series and high voltage decoupling is internal to the stack.
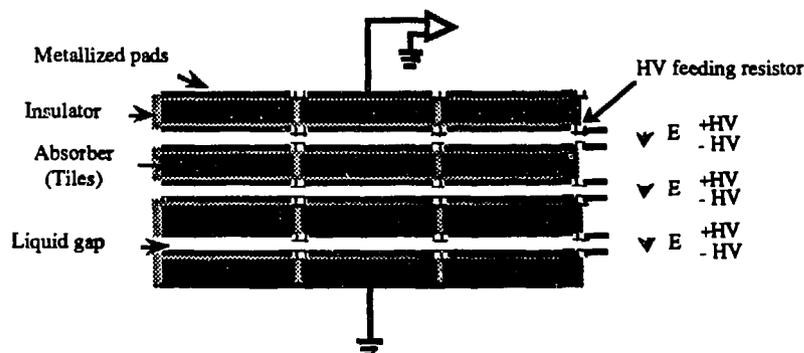

Figure 5. EST design which avoids cumulative high voltage. High voltage is fed in parallel, signal is readout in series. Low inductance high voltage decoupling is internal to each electrode.

4.2 Tower crosstalk.

Figure 6 shows schematically the sources of crosstalk from a central tower to eight surrounding towers. A fraction of the charge produced in each gap is capacitively coupled to neighboring towers. For a large area hadronic tower, this is a small part of the total, i.e. $c/C \ll 1$; but because the transformer action reduces the total capacitance, the importance of crosstalk increases with the transformer ratio.
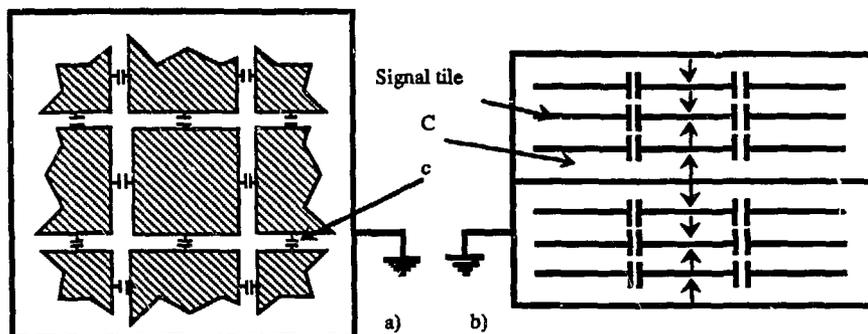

Figure 6. Plan and elevation schematics showing sources of crosstalk between towers of an EST of transformer ratio 2. C is the capacitance of each gap within a tower; c is the coupling capacitance of each tile to a nearest neighbor. Each calorimeter module of many towers is in a grounded container. Within each tower the signal tiles and ground plates are summed along a low impedance transmission line (not shown).

4.2.1 Test set-up

To carefully tevaluate he detailed electrical properties of a calorimeter based on EST, we have constructed the aluminium model of figure 7 and simulate its response assuming that it could be described by the schematic shown in the same figure.
The central reference tower is surrounded by eight neighbors, of which four are nearest neighbors. The entire section of calorimeter is inside a grounded box. Tiles are made of aluminium, 6" x 6" in area and 3/8" thick; sensitive gaps are replaced by air gaps; gap size is fixed at 2mm; these numbers have been chosen to simulate what could be the size of a tower in a realistic hadronic calorimeter. With access from the top, the number of tiles between each signal tiles and the two ground planes is changed in order to vary the transformer ratio n; the number of gaps in the structure is 2 x n; the two sets of n gaps being in parallel. For a transformer ratio of 5 (10 gaps), the structure corresponds to approximately 1/4 the thickness of a high Z tower which is two absorption lengths thick. The crosstalk capacitance c is varied by changing the spacing between towers from 1/16" to 1/2".
The central tile of each tower, which collects the signal from both subsections, is connected to an integrating preamplifier ($\approx 50\,\Omega$ input impedance) by a rod in a hole through the upper subsection. To simulate the entire calorimeter stack (40 gaps) an external discrete capacitance is connected in parallel with the preamplifier input. Current from drifting electrons in any gap of the reference tower are simulated using a high impedance probe inserted through a hole in the lower subsection. The current waveform corresponds to that of the ionization current shown in figure 1 with a drift time of 100 ns. Actually, the probe current flows between a given tile and ground; the effect of a current source in a single gap is obtained by taking differences.
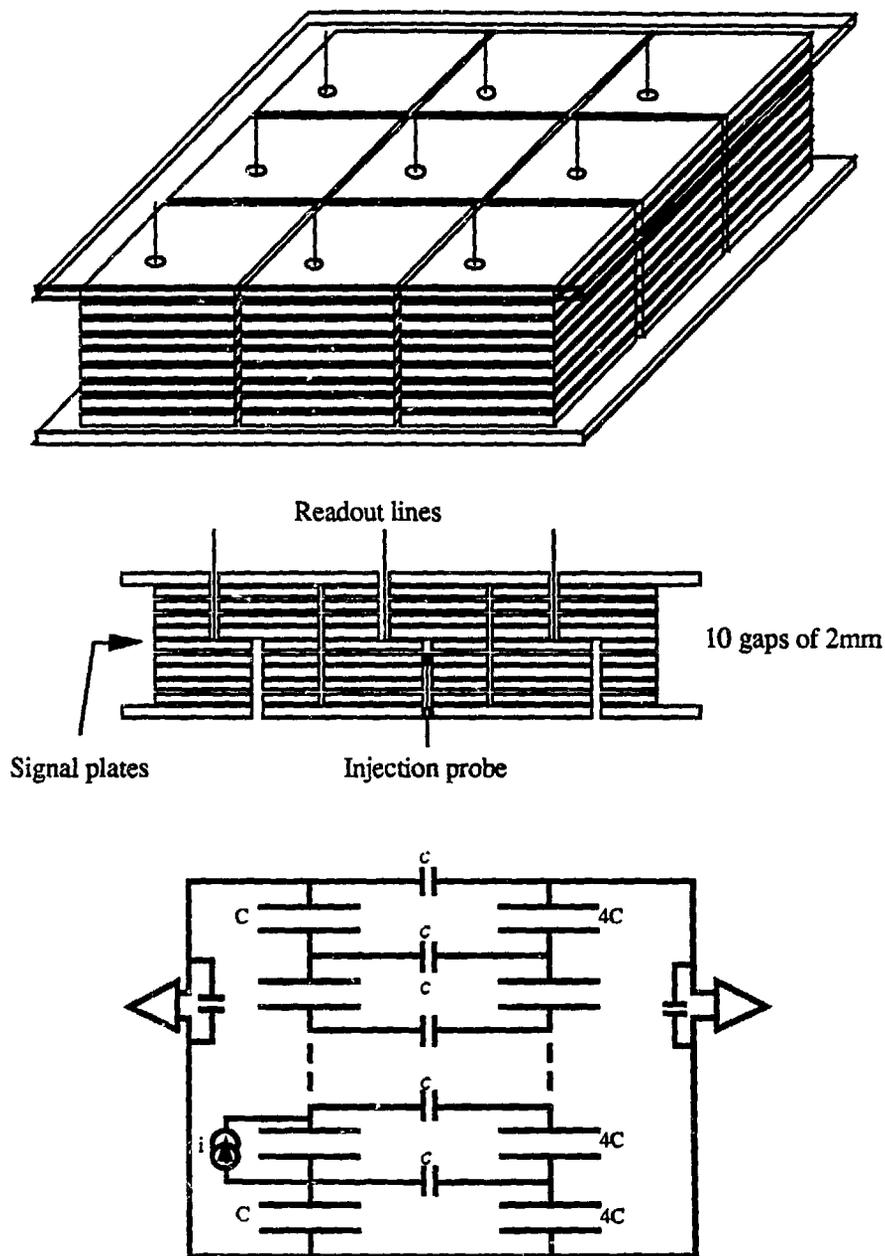
8

EST Aluminium model

Figure 7. Aluminium model to study the EST pulse properties. The set-up consists of nine towers. Each tower is made up of two parallel sets of gaps; each set with 1 to 5 gaps. Aluminium tiles are 6"x6" in area and 3/8" thick; sensitive gaps are filled with air; gap size is fixed at 2mm; tower spacing can be varied from 1/16" to 1/2" to study the influence of the coupling capacitance. The electrical schematic shown is used to simulate the pulse response of the model. The gap capacitance C is 100 pF; the coupling capacitance c is 15 pF.

4.2.2 Measurement results

All measurements on the aluminium model are well reproduced by the simulation of the electrical circuit in figure 7. This simple circuit diagram enables us to understand what's going on and to extrapolate to other configurations. The main results can be summarized as :

i-   The tower capacitance decreases as the transformer ratio increases; this translates into a much faster rise-time at the preamp-output, from ≈ 1µs when all gaps are in parallel to less than 50 ns for a transformer ratio of 5 (see figure 8b where pulse rise time is actually dominated by the input signal 100 ns drift time).

ii- Whatever the injection gap and the tower spacing, summing the 9 towers we get the total charge injected. Crosstalk means loss of localization not of energy.

Test Pulse

c)

100 ns

a)

b)

Test Pulse on gap 1 alone

central tower 20mV/20ns

side tower 2mV/20ns

Test Pulse on gaps 1 to 5
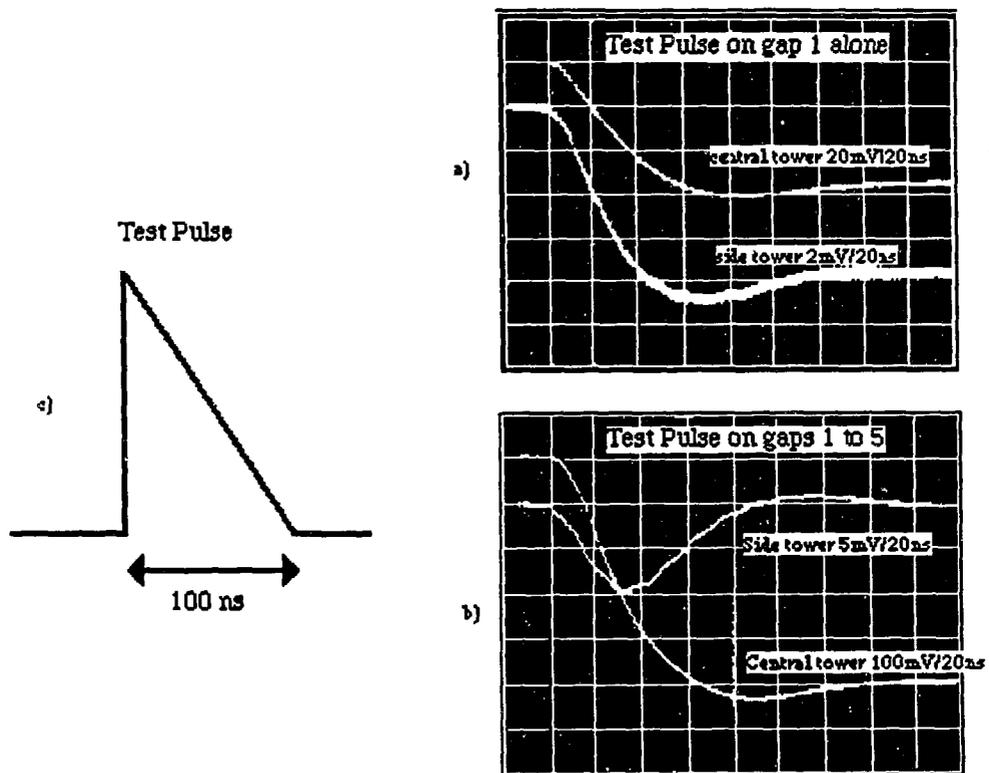
Side tower 5mV/20ns

Central tower 100mV/20ns

Figure 8. Preamp output pulses of central and side towers when the test pulse shown in c) is fed into the structure. Transformer ratio is 5, and tower are spaced by 1/8". In a) gap 1 only is pulsed; in b) all gaps 1 to 5 are pulsed together.

10

iii- Crosstalk in the adjacent towers behaves in two qualitatively very different ways
whether a signal is sent in only one gap or whether the same signal is applied to all
the gaps. Figure 8a shows the preamplifier outputs of the reference tower and of a
side tower when only one gap (that which is closer to the ground plate) is pulsed.
Tower spacing is 1/8" and transformer ratio is 5. The crosstalk signal tends to a non
zero value at large time. On the contrary, crosstalk tends to zero when all gaps are
pulsed identically (figure 8b). This feature is well reproduced by the simulation
and can be understood considering that in the case of equal currents in all gaps, no
charge can accumulate at the intermediate tiles and that the only source of crosstalk
is the non zero input impedance of the preamplifiers which produces a short pulse at
small time.

Analytic analysis of the electric circuit of figure 7 shows that crosstalk depends
on the ratio c/C of the coupling capacitance to the gap capacitance. Results obtained
with this air gap model are then valid for a liquid calorimeter. This tells also that the
larger the tile area (~ C) compared to its perimeter (~ c), the better. The domain of
validity of this scheme is well matched to large hadronic towers.

To be quantitative, let's define crosstalk as :

χ = signal in one side tower / sum over the 9 towers

where signal is measured at 200ns. Crosstalk measurements for two tower spacings
are compared with the simulation results in the table below :

Injection in gaps #	χ (1/4" spacing) measured	χ (1/8" spacing) measured	χ (c/C = .15) computed
1	.065	.10	.095
1-2	.055	.09	.085
1-2-3	.045	.075	.067
1-2-3-4	.027	.047	.040
1-2-3-4-5	0.	0.	0.

Note that the coupling strength c/C = .15, which enables us to reproduce the 1/8"
spacing measurements, corresponds precisely to the estimated side capacitance
between adjacent towers (16 pF / 100 pF) for that spacing.

In addition, as expected, crosstalk values decrease when transformer ratio is
decreased. The table below shows, for various transformer ratios and two tower
spacings, the measured crosstalk when the gap closer to the ground plate is pulsed.
Again, although not shown,measurements results agree well with simulation.

transformer ratio	χ (1/4" spacing)	χ (1/8" spacing)
5	.065	.100
4	.045	.070
3	.027	.045
2	.013	.017

The same data enables us to study variation in the collection efficiency of the gaps ganged in series. Let's define ε_i the collection efficiency of gap i as :

$$\varepsilon_i = \frac{S_i}{\frac{1}{n}\sum_1 S_j}$$

where Si is the signal when gap i is pulsed alone, n is the transformer ratio and gap 1 is that closer to the ground plane. Measurements for a 1/4" spacing yield :

gap #	n = 5	n = 4	n = 3	n = 2
1	.73	.78	.87	.93
2	.76	.86	.95	1.07
3	.88	1.02	1.18	-
4	1.12	1.34	-	-
5	1.52	-	-	-

To interpret these numbers, let's consider a case where the gap currents are equal and compute the sensitivity of the output signal S to a variation of current i in gap k. It is easy to find out that we have :

$$\frac{\Delta S}{S} = \frac{\Delta i}{i} \times \frac{\varepsilon_k - 1}{n-1}$$

For instance, a 10% variation of the current in gap 1 relative to the average current in 5 gaps connected in series, change the output signal by only .7%. Through fluctuations in the longitudinal shower development, this effect will slightly degrade the energy localisation of the calorimeter. In a model where in all gaps, the current is the same in average, but fluctuates independently in each gap, the error introduced by the non uniformity in the gap collection efficiency is zero on average but gives rise to an additional fluctuation on the energy seen by the central tower :

$$\frac{\sigma(S)}{S} = \frac{\sigma(i)}{i} \times \frac{\sqrt{\sum_{l=1}^{n} (\varepsilon_l - 1)^2}}{n}$$

The error on the output signal fluctuates as the current in each gap but the fluctuation is reduced by an amount which varies from ≈ 25 for a small transformer ratio of 2 to ≈ 10 for a transformer ratio of 5. Hence, this contribution to the energy localisation is probably acceptable. Nevertheless, a detailed shower simulation must be made to have quantitative numbers. Note again that the energy unseen in the central tower will be detected in the adjacent cells.

This first study of the EST gives promising results. It indicates that crosstalk will be small even for relatively large transformer ratios, provided that the series connection is over a length small compared to a shower length, the ionization signal will then be nearly equal in all gaps. The effect of the variation in gap collection efficiency on the energy resolution has to be better quantified but is probably acceptable at least for hadronic calorimeters where the EST approach is the most useful.

5. Signal processing and pile-up.

When after $\approx$ 15 ns, the next collision comes in, electrons drifting in the ionization gap are not all collected. These remaining electrons induce some pile-up from one event to the next. This can be zeroed on average if the time averaged value of the output signal is zero using AC coupling for instance. However, there is still a random fluctuation in the base line which will affect the energy measurement.

To be quantitative, let us consider a preamplifier with an exponential rise time with a time constant $T_m/2$. This preamplifier is AC coupled to remove any DC shift in the base line but this is achieved with a much longer time constant of several microseconds. The preamplifier output P(t) is processed through one or the other of the two following filters :

$$F_1(t) = P(t) - P(t-T_m)$$
$$F_2(t) = P(t) - 2P(t-T_m) + P(t-2T_m)$$

Time 0 is the crossing time. T_m the measurement time is the time where the signal is measured. Figure 9 sketches the different waveforms. As explained in reference 1, the idea behind filter 2 is that if T_m is much smaller than the drift time, this processing will cancel the tail of the pulse.
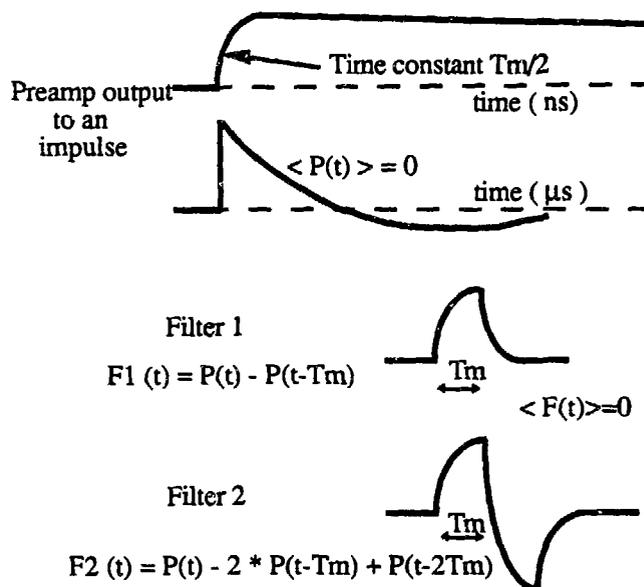

Figure 9. Preamplifier and filter waveforms used to estimate pile-up and signal to noise performances.

The response at time T_m of the filter F to a triangular shaped current wave form originating at time t_i is:

$$S(t_i) = \int_{t_i}^{min(t_i+t_d,T_m)} (1-\frac{t}{t_d}) \times F(T_m-t) \times dt$$

The probability for a cell to be hit is : $p = \dfrac{L \times \sigma \times N_p}{N_{cell}}$

L, the luminosity, is assumed to be $10^{33} cm^{-2} s^{-1}$, σ the cross-section is 100 mbarn. Each of the particles (N_p =100 in average) has a mean energy $<E_t>$ of 0.5 GeV. The calorimeter is assumed to have 25 000 cells (N_{cell}) which correspond to a segmentation $\Delta\eta \times \Delta\phi = .05 \times .05$ over the whole rapidity region $|\eta| < 4$.

The average value of pile-up: $p \times <E_t> \times \sum_{t_i < T_m} S(t_i)$ is zero as advertised above because $<P(t)>$ is zero.

In the limi. ... re the probability p for a cell to be hit is small, the random fluctuation in the base-line of this cell has an R.M.S. :

$$<E_t> \times \sqrt{ p \times \delta \times \sum_{t_i < T_m} S(t_i)^2 }$$

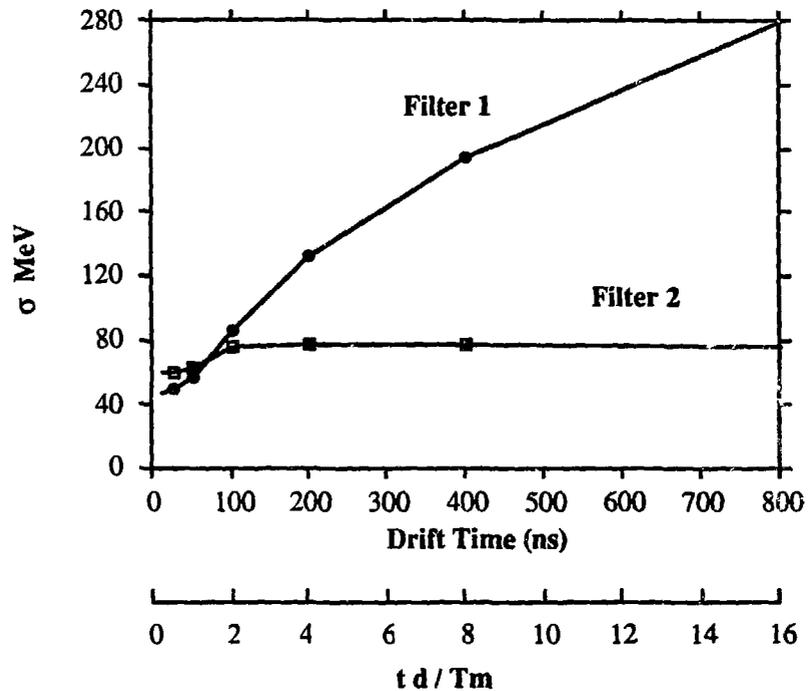where δ is the time between bunches : 15 ns.

Figure 10. Pile up contribution to the error on the transverse energy measurement in a single cell as a function of the drift time. The strong bipolar shaping is quite effec'ive at reducing the pile up for long drift times. Both filters are similar for short drift times : less than .....e the measurement time.

Assuming a measurement time T_m of 50 ns, figure 10 gives the estimated noise contribution to the transverse energy from pile-up as a function of the electron drift time t_d in liquid. Filter 2 does its job of canceling the tails of the pulse. The contribution to the noise is constant at $\approx$ 80 MeV for each calorimeter cell. This not true for filter 1

14

where to keep pile up at an acceptable level, we have to stay at short drift times $t_d/T_m < 2$.

In summary, long drift time is not a real problem for pile-up. Tails can be effectively removed by fast bipolar shaping. However as we will see below, the price to pay is a noise increase of ≈ 1.7. So if possible it is better to stick to a moderate drift time, i.e. a drift time less than or equal to twice the measurement time; there the simpler shaper #1 is quite adequate from a pile-up point of view and gives a better signal to noise ratio.

6. Signal and electronics noise in liquid ionization calorimeters

6.1 Minimum ionizing particle signal.

When a minimum ionizing particle (M.I.P.) goes through the calorimeter, each gap gives a triangular current pulse as explained in 2 with a peak current I_{max}. This pulse is processed by the filters defined in section 5. the signal collected is :

$$Q_{collected} = N_{gap} \times I_{max} \times S(0) = N_{gap} \times I_{max} \times T_{eff}$$

The filter response at time Tm to a particle crossing the gap at time 0 : S(0) (see section 5) can be looked at as an effective integration time T_{eff}. Its value is shown in figure 11. For a measurement time T_m large compared to the drift time t_d the effective integration time is $t_d/2$. the factor 2 reflects the triangular shape of the current pulse. If however, as will happen in an SSC calorimeter T_m is small compared to t_d then T_{eff} approaches the measurement time T_m but does not quite get to it due to the finite rise time of the preamplifier pulse. At this point, the signal does not depend any more on the size of the gap.This occurs for a drift time greater than about twice the measurement time.
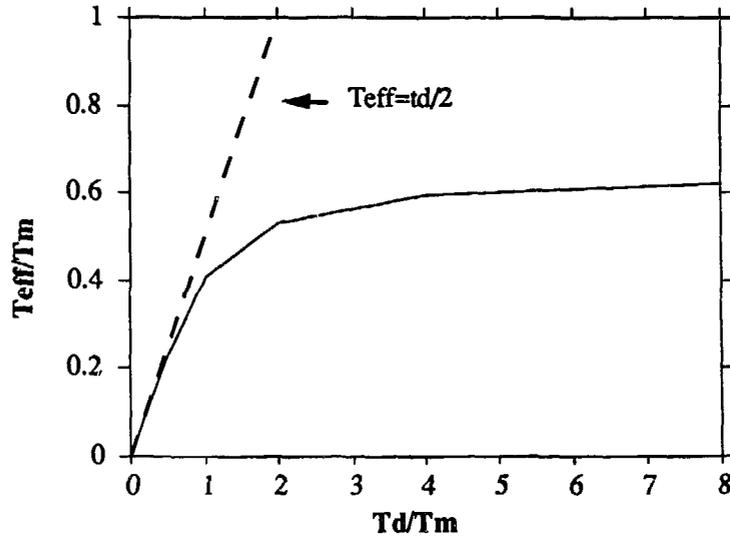

Figure 11. Effective integration time for a given measurement time T_m as function of the drift time. The effective integration time is long enough to get the whole charge (td/2) only when the drift time is small compared to the measurement time. In the other extreme, the effective integration time approaches a constant set by the measurement time and does not depend upon the gap size any more.

15

6.2 Noise

Electronic noise at fast shaping time is dominated by the series noise of the input FET of the preamplifier. For a given preamplifier, it is well known that this noise is proportional to the capacitance which loads its input. If we optimize the preamplifier to the detector then the optimal noise goes like the square root of the detector capacitance C_D. More precisely, following reference 1

$$ENC = \frac{4}{\sqrt{3}} I_s \sqrt{kT} \sqrt{\frac{\tau_A}{T_m}} \sqrt{C_D}$$

τ_A is the amplifier time constant and is of order 2 ns. I_s is the series noise integral :

$$I_s = \sqrt{T_m \int_0^\infty F(t)^2 \, dt}$$

For filter 1 I_s is 1.52 and 2.57 for filter 2. As mentioned in section 5 the strong bipolar filter #2 is noisier by $\approx$ 1.7 than filter #1.

6.3 Signal/Noise and optimum gap thickness

Let's now consider a calorimeter with a fixed thickness of liquid L subdivided in a number of gaps each of a variable width g. The number of gaps, Ngap, is L/g. In an hadronic calorimeter, the capacitances are large and we will neglect the capacitance of the connections in this computation which aims mainly at comparison. For a pad surface area A, the detector capacitance C_D is (all gaps connected in parallel)

$$C_D = \alpha \times N_{gap} \times \frac{A}{g}$$

where α= 14.2 pF/m for Liquid Argon and 17.8 pF/m for TMP/TMS taking into account the difference in dielectric constants.

Collecting previous results, the optimum signal to noise ratio reads :

$$\frac{S}{N} = \beta \times I_{max} \times (\frac{T_{eff}}{T_m}) \times T_m^{3/2} \times \sqrt{\frac{L}{A}}$$

β is 2.5 $e^{-1}\sqrt{\frac{s}{m}}$ for liquid Argon with filter #2 and 3.8 $e^{-1}\sqrt{\frac{s}{m}}$ for TMP/TMS using filter #1.

The only gap dependence is through the ratio T_{eff}/T_m which as noted in section 6.1 tends to a constant as soon as the gap is wide enough that the drift time is more than twice the measurement time. On the other hand, minimization of pile-up and of the sampling fluctuations require a small gap. As a reasonable compromise, we choose a liquid gap such that $t_d = 2 T_m$. For sake of illustration, for a 50 ns measurement time this would correspond to a 0.5 mm gap for liquid argon (as advocated in ref. 3), 1.2 mm gap for TMP at 40 kV/cm, 2 mm for TMS at 20 kV/cm.

Note also, as already underlined in section 2, that the signal to noise ratio depends on the peak current I_{max} and not on the total charge. Figure 12 shows a comparison of peak current for various liquid as a function of the drifting electric field. For room temperature liquids data at low electric field are from Holroyd [7]. Values of

G_{fi} at higher fields have been obtained using the Onsager relation given in [8]. At 50 kV/cm TMP has the same peak current as liquid argon. The cross-over between liquid argon and TMS is at the much lower field of 20 kV/cm.

The strong noise dependence on the measurement time T_m, once the gap width has been optimized, is also made explicit. Increasing the measurement time from 50 ns to 100 ns would reduce the noise by as much as a factor 2.8.
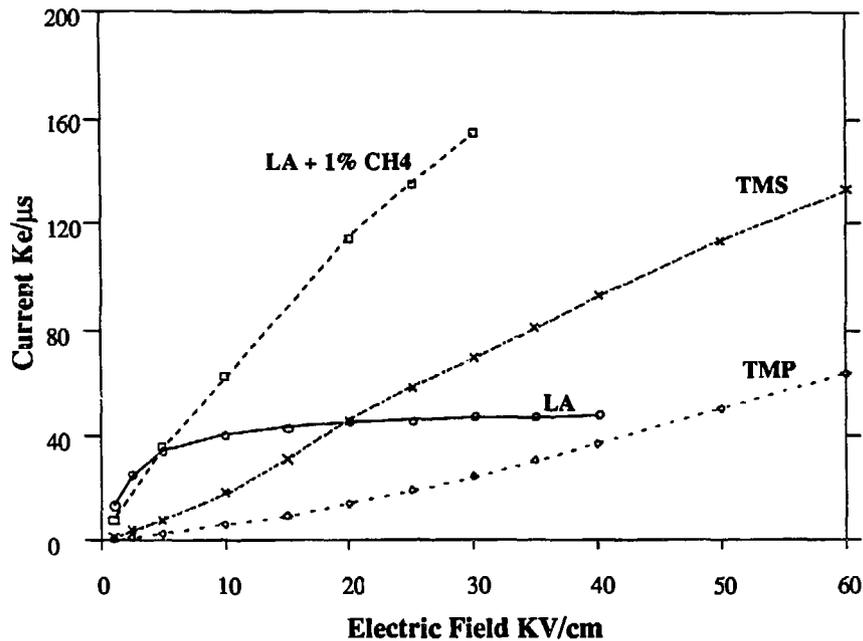

Figure 12. Peak current as a function of electric field.

6.4 Signal/Noise for TMP/TMS compared to liquid argon

For the sake of the comparison let's consider a fast calorimeter with a 50 ns measurement time. The total liquid thickness is fixed at 300 mm. For liquid argon assuming that due to cryogenics problem it is more difficult to build a small gap, this one has been fixed at 2mm. The electric field is set at the standard value of 10 kV/cm. The drift velocity is saturated and the drift time is 400 ns. To keep pile up at an acceptable level we have to use the strong bipolar filter #2 as discussed in section 5. In the case of warm liquid, we will study the noise as a function of the applied electric field. The gap will be varied accordingly to keep the drift time at 100 ns, twice the measurement time. We can then use filter #1. The pile up will be about the same as in the liquid argon case due to the faster drift time. Assuming a 10 x 10 cm2 pad size and collecting results from the previous sections we end up with the results shown in figure 13.

In such devices, M.I.P. can be seen above noise. However the full length of liquid is needed. In the liquid argon case M.I.P. will not be seen in each of the individuals samplings in depth. As the electric field increases, performance of TMP and TMS improves. At 15 kV/cm TMS is as good as liquid argon. TMP has to run at the higher voltage of 37 kV/cm to catch up with liquid argon. The reason for this improvement with electric field is twofold: The peak current increases because the free ion yield increases with electric field and mainly because the drift velocity increases. In

addition, this larger drift velocity allows a larger gap for a fixed drift time reducing the detector capacitance and thus the noise. However practical limitation on the high voltage that can be used makes TMS a much better candidate than TMP if safety issues related to this liquid can be handled.
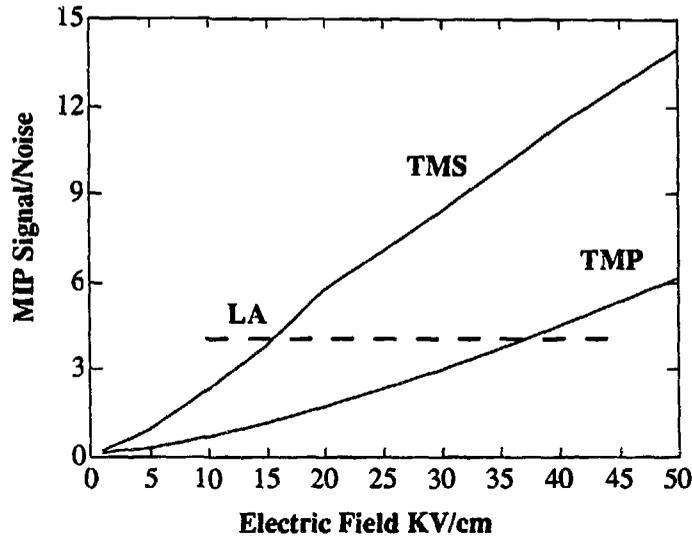

Figure 13. Signal to noise ratio for a minimum ionizing particle as function of the electric field for a measurement time of 50 ns. The pad size is 10cm x 10cm and the liquid depth is 300mm. For TMP/TMS the gap width is varied with high voltage such that the drift time is held at 100ns. Liquid argon is there for comparison; the gap is fixed at 2mm the electric field is 10kV/cm

Let's define the absorber of the calorimeter to translate the noise figures above in unit of energy. Choose 1.2 meters of lead as absorber. This provides for seven collision lengths to absorb hadronic showers. The absorber to detector thickness ratio is 4, which should give compensation i.e same signal response for hadronic electromagnetic showers. A M.I.P. will deposit by ionization 1.6 GeV in the calorimeter but only 3% in the liquid. Electron and hadrons signals are depressed with respect to muon signals. Assuming ratios $e/\mu=0.6$, $e/h=1$, the M.I.P signal corresponds to the energy deposited by a 2.6 GeV shower. The noise figures then read :

Liquid	gap (mm)	Voltage per gap (kV)	Electronic noise GeV/m2	Pile up noise on transverse energy @10**33 GeV/m2
Liquid Argon	2	2	6.5	.52
TMP@40kV/cm	1.2	4.8	5.8	.56
TMS@20kV/cm	2	4	4.6	.56

These numbers are much larger than we are used to at longer measurement times and reflect the strong time dependence underlined in 6.3. There are probably good enough for the high energy calorimeters will have to measure at SSC.

18

7. Conclusion

Although liquid ionization calorimeters have been mostly used up to now with slow readout, their signals have a fast rise time. However, it is not easy to get this fast component of the pulse out of the calorimeter. A careful design of the electrodes and of their connections is necessary. A measurement time, i.e. the time between the bunch crossing time and the time when the actual measurement is made, of 50 ns is probably achievable. Pile up contribution to the error in the energy measurement should not be too important for such a short shaping time.

One way to achieve that result is to follow the route pioneered by the Helios collaboration and to use ferrite transformers and preamplifiers buried into the liquid. One other solution might be to use the Electrostatic Transformer approach to keep the detector capacitance low while keeping the number of channels at a reasonable level. This solution allows for the use of transmission lines between the detector and the preamplifiers which can then be located in an accessible area. These cables should be kept short to minimize the added noise. This seems feasible in a room temperature liquid calorimeter.

For fast calorimetry, the signal to noise ratio for room temperature liquids is comparable to or better than the one obtained with liquid argon, at the expense of a slightly higher gap voltage. TMS with its higher drift velocity is very attractive if safety issues can be handled.

In all cases, the electronic noise at the very short shaping times considered in this paper is much larger than what has been obtained with the existing calorimeters using a much longer readout time. This is probably acceptable at SSC where the physics interest is more at the 100 GeV scale.

Acknowledgements

References

1- Speed and Noise Limits in Ionization Chamber Calorimeters
V. Radeka and S. Rescia.
Nucl. Inst. and Method A225 (1988) 228-242

V. Radeka.
Proceedings of the 1987 SLAC instrumentation conference

2- Experiment NA34 at CERN

3- Noise and Pile-up in Liquid Sampling Calorimeters
P. Franzini
Proceedings of the 1987 Workshop on Experiments, Detectors and Experimental areas for the Supercollider

4- Fast Hermetic Calorimetry Using Warm Liquids
Proposal for Generic Detector R&D for the SSC/LHC

LBL-09-1987
WALIC collaboration

5-   Saturation of ionization signal in TMP and TMS at different angles and electric fields.
B. Aubert et al.
LAPP-EXP/89-08
to be published in NIM

6-   Purity in room temperature liquid ionization chambers
S. Ochsenbein, D. Schinzel, A. Gonidec, W.F. Schmidt
Nucl. Inst. and Method A273 (1988) 654-656

Purification de 12000 litres de TMP pour l'expérience UA1 au CERN
A. Gonidec
Journée d'études sur la conduction et le claquage dans les isolants liquides
28-29 Septembre 1989, Toulouse

7-   The Physics and Chemistry of Room-Temperature Liquid Filled Ionization Chambers
R. A. Holroyd and D. F. Anderson.
Nucl. Inst. and Method A236 (1985) 294-299

8-   Performance of a Uranium/TMP Electromagnetic Calorimeter
UA1 Collaboration, M. Albrow et al.
Nucl. Inst. and Method A236 (1985) 294-299

On the Measurements of Electron and Positive Ion Mobilities in Liquid TMP
A. Gonidec et al.
UA1/TN 87-66

Analysis of the Signal Produced by Cosmics Rays in Liquid TMP
C. Bacci et al.
UA1/TN 86-85

9-   Drift velocities of excess electrons in 2,2,4,4-TMP and TMS :
a fast technique
H. Faidas et al.
Submitted to Chemical Physics Letters

10-   Report of the Large Solenoid Detector Group
Proceedings of the 1987 Workshop on Experiments, Detectors and Experimental areas for the Supercollider

11-   Electrostatic Transformers for Large Towers
J. Colas and W.A. Wenzel
Proceedings of the Workshop on Calorimetry fo the Superconducting Super Collider
March 13-17, 1989, Tuscaloosa, Alabama